Buletin Ilmiah Sarjana Teknik Elektro
Vol. 8, No. 5, October 2026, pp. 1724-1740
ISSN: 2685-9572, DOI: 10.12928/biste.v8i5.16115

Optimal Controller Design for Doubly Fed Induction Machines Using Advanced Genetic Algorithm

Habib Chaib [1], **Belkacem Belabbas** [1], **Fajer M. Alelaj** [2], **Housseyn Chaib** [1], **Mohamed Metwally Mahmoud** [3,4,5]

[1] Department of Electrical Engineering, Laboratory of Electrical Engineering and Plasmas, University Ibn Khaldoun, Tiaret, Algeria
[2] Water Research Center, Kuwait Institute for Scientific Research, Kuwait
[3] Department of Electrical Engineering, Faculty of Engineering, Aswan University, Aswan 81542, Egypt
[4] Jadara University Research Center, Jadara University, P.O Box 733, Irbid, Jordan
[5] ENET Centre, CEET, VSB—Technical University of Ostrava, Ostrava, 708 00, Czech Republic

ARTICLE INFORMATION

Article History:

Received 07 March 2026
Revised 31 May 2026
Accepted 12 November 2026

Keywords:

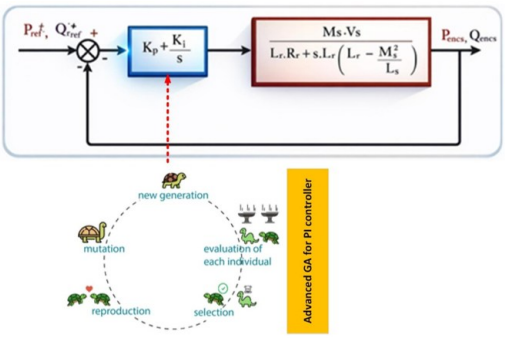
Advanced Genetic Algorithm;
Doubly-Fed Induction Machine;
Optimized Controller;
Energy Control;
Electric Machines

Corresponding Author:

Mohamed Metwally Mahmoud,
Department of Electrical Engineering,
Faculty of Engineering, Aswan University, Aswan 81542, Egypt
Email: metwally_m@aswu.edu.eg

This work is open access under a Creative Commons Attribution-Share Alike 4.0

ABSTRACT



The primary objective of this article is to enhance the PI controller performance in stator-flux-oriented vector control applied to a DFIM by leveraging GAs. The efficiency and robustness of the DFIM, widely used in applications such as WECSs, depend significantly on the precise tuning of its control parameters. Conventional methods for tuning PI controllers often fall short in achieving optimal performance due to the complex and nonlinear nature of DFIM dynamics. GAs, inspired by the principles of natural selection, offer a powerful optimization framework capable of navigating complex search spaces to identify near-optimal solutions. In this study, we develop and implement a GA-based approach to optimize the PI gains for the stator-flux-oriented vector control strategy. The proposed methodology aims to improve dynamic response, minimize steady-state errors, and enhance system stability under varying operating conditions. Simulation results demonstrate the effectiveness of the GA-tuned PI controllers in comparison with Ziegler-Nichols tuned controllers. The proposed approach not only achieves superior performance metrics but also reduces the computational effort required for parameter tuning. The findings underscore the potential of genetic algorithms as a valuable tool in advancing control strategies for high-performance electrical drive systems.

Document Citation:

H. Chaib, B. Belabbas, F. M. Alelaj, H. Chaib, and M. M. Mahmoud, "Optimal Controller Design for Doubly Fed Induction Machines Using Advanced Genetic Algorithm," *Buletin Ilmiah Sarjana Teknik Elektro*, vol. 8, no. 5, pp. 1724-1740, 2026, DOI: 10.12928/biste.v8i5.16115.

1. INTRODUCTION

The global transition toward clean and sustainable energy has significantly increased the deployment of wind energy systems, making wind power a key contributor to future carbon-neutral power grids [1]-[5]. Despite its advantages, the large-scale integration of WECS introduces challenges related to power quality, grid stability, and harmonic distortion due to the intermittent nature of wind resources and the use of power electronic converters. These issues can negatively affect voltage stability, power factor, and connected equipment reliability. Consequently, enhancing the dynamic performance and power quality of WECS has become a major research focus, particularly for systems employing DFIMs, which are widely adopted for variable-speed wind turbine applications [6]-[8].

HAWTs dominate the renewable energy landscape due to their high efficiency and scalability. Their design, characterized by a rotor mounted on a horizontal shaft and typically positioned upwind of the tower, allows for maximum energy capture from wind resources [9]-[11]. The operation of HAWTs, however, demands sophisticated control mechanisms to ensure efficiency and reliability, particularly under varying wind conditions. Among the various types of generators used in WT systems, the DFIM is a preferred choice for its ability to operate efficiently over a wide range of wind speeds and its capability to perform MPPT. This feature, combined with its reduced converter size compared to fully-rated converters, makes the DFIM a cost-effective solution for grid-connected WTs [12]-[14].

Other generator systems, such as SCIG and PMSG, present alternative solutions but come with limitations. SCIGs lack the flexibility to operate efficiently over a wide speed range without additional equipment, while PMSGs often require higher initial investment due to their dependency on rare-earth materials. The DFIM strikes a balance, offering flexibility, efficiency, and cost-effectiveness, making it a favored choice for large-scale wind energy applications [15]-[18]. The operational zones of a wind turbine are typically divided into regions to optimize performance. The MPPT zone, in particular, ensures maximum energy extraction from wind resources by adjusting the generator speed to match the optimal tip-speed ratio. Control strategies, such as stator-flux-oriented vector control, are instrumental in achieving this objective, providing the precision and adaptability required for efficient operation [19]-[22].

This article provides a state-of-the-art review of WT control strategies with a focus on DFIM applications. By addressing the challenges and limitations of existing methods, we aim to highlight the advantages of genetic algorithms in enhancing control performance and ensuring sustainable energy generation. Numerous studies have explored control strategies and optimization techniques for wind energy systems. In the context of DFIM, traditional PI controller tuning methods have been widely implemented due to their simplicity and ease of deployment. However, these methods often result in suboptimal performance, particularly under varying operating conditions and nonlinear dynamics inherent to wind turbines [23]-[26], .

Recent research has highlighted the potential of advanced optimization algorithms in addressing these challenges. For instance, PSO and FLC have been applied to enhance PI controller tuning, showing improvements in dynamic response and stability. Despite these advancements, these techniques can be computationally intensive and may struggle with high-dimensional optimization problems [27]-[29]. GAs has emerged as a promising alternative, offering robust performance in nonlinear and complex optimization landscapes [30]-[33]. Studies have demonstrated the effectiveness of GA-based tuning in improving control accuracy and reducing steady-state errors. For example, previous works have successfully applied GAs to optimize control parameters in PMSG-based systems, achieving significant gains in energy efficiency and reliability. For a literature review, it is often useful to summarize recent optimization-based control and parameter tuning methods applied to DFIMs in a comparative table. Table 1 highlights the optimization technique, control objective, and major findings from representative recent studies.

The paper is organized as follows. Section 2 describes the HAWTs based on the DFIM model and its control. The indirect vector control with power loop and the optimal design of PI controllers using GAs are presented in Section 3. Simulation results and discussions are detailed in Section 4, followed by the conclusion in Section 5.

Table 1. Summary of recent optimization-based studies on DFIMs

Ref.	Method	Application	Main Objective	Key Findings	Limitations
[34]	GA	PI controller tuning for RSC	Improve speed and power regulation	Enhanced dynamic response and reduced settling time compared to conventional tuning	Computationally intensive for large search spaces
[35]	PSO	Vector control parameter optimization	Minimize active/reactive power fluctuations	Faster convergence and improved robustness under wind variations	May suffer from premature convergence
[36]	GWO	DFIM controller gain optimization	Reduce overshoot and tracking error	Better global search capability than PSO in some scenarios	Performance depends on parameter selection
[37]	WOA	MPPT and controller tuning	Maximize energy extraction and improve stability	Achieved higher power capture efficiency	Convergence speed can vary with operating conditions
[38]	ACO	Parameter identification of DFIM	Improve machine model accuracy	Accurate estimation of machine parameters	Higher computational burden
[39]	DE	Optimal tuning of current controllers	Enhance transient performance	Strong optimization capability with good robustness	Requires careful setting of mutation parameters
[40]	ABC	Power control optimization	Minimize steady-state error	Improved power quality and reduced oscillations	Slower convergence than some modern metaheuristics
[41]	HHO	PI/PID gain tuning	Improve fault ride-through performance	Superior exploration–exploitation balance	Limited industrial validation
[42]	MPA	Multi-objective DFIM control	Simultaneous optimization of speed and power responses	Better compromise among conflicting objectives	Relatively new with limited comparative studies
[43]	Hybrid GA–PSO	Controller parameter optimization	Combine global and local search abilities	Improved convergence and control performance	Increased algorithm complexity

2. MATERIALS AND METHODS

2.1. Configuration and Modelling of the HAWTs

The process of extracting the kinetic energy contained in the wind is explained by Betz's theory. The WT structure is seen in Figure 1. This theory leads to the determination of the WT power [44]-[47]:

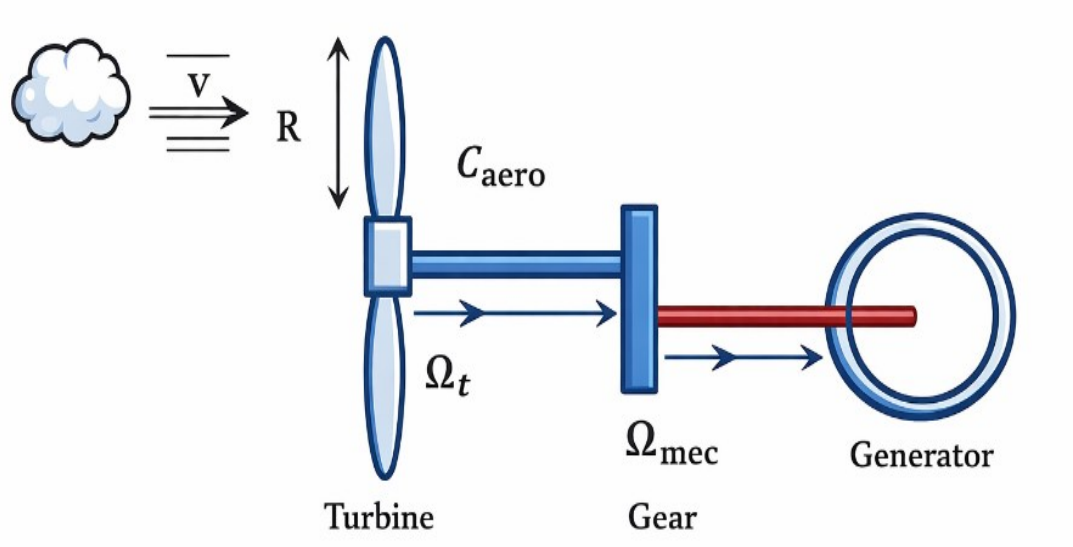


Figure 1. Diagram of the WT

The aerodynamic power P_{aer} at the WT rotor is expressed as follows [48][49]:

$$P_{aer} = C_p P_V = \frac{1}{2} C_p(\lambda, \beta) \rho s v_v^3 \quad (1)$$

Where C_p is a function of β and λ :

$$\lambda = \frac{\Omega_t \, R_t}{V} \tag{2}$$

The C_p has been approximated, for this type of turbine, by the following equation [50][51]:

$$C_p(\lambda, \beta) = C_1 * \left(C_2 * \frac{1}{\lambda_i} - C_3 * \beta - C_4\right) * e^{-\left(\frac{-C_5}{\lambda_i}\right)} + C_6 * \lambda \tag{3}$$

with :

$$\frac{1}{\lambda_i} = \frac{1}{\lambda + 0.008 * \beta} - \frac{0.035}{1 + \beta^3} \tag{4}$$

The C_p represents the aerodynamic efficiency of the WT. The six coefficients defined, depend on the specific WT and are presented in Table 2:

Table 2. Coefficients defining the evolution of C_p

Coefficient	Value
C1	0.5176
C2	116
C3	0.4
C4	5
C5	21
C6	0.0068

Knowing the speed of the WT, the C_{aer} is therefore directly determined by [52]:

$$C_{aer} = \frac{P_{aer}}{\Omega_t} = \frac{1}{2}\frac{1}{2} C_p(\lambda, \beta) \rho s v_v^3 \frac{1}{\Omega_t} \tag{5}$$

The principle of MPPT is one of the various methods for regulating the electromagnetic torque (and consequently the converted electromagnetic power) to improve the mechanical speed and the electrical power produced. The wind speed is stochastic and highly fluctuating. These variations are the main disturbance in the wind conversion chain, leading to power fluctuations. The electrical machine and its inverter are perfect, meaning that, regardless of the power generated, the electromagnetic torque developed is always equal to its reference value [53].

$$C_{em=} C_{em-ref} \tag{6}$$

Determining the WT speed allows for obtaining the MP generated in MP extraction techniques. The application of three torques: a wind torque, an electromagnetic torque, and a resisting torque, influences the speed, as we have already explained. By combining the action of these three torques, only two torques govern the mechanical speed, namely the torque from the gearbox C_g and the electromagnetic torque C_{em} [54].

$$\frac{d\Omega_{mec}}{dt} = \frac{1}{j}(C_g - C_{mec} - C_{em}) \tag{7}$$

The control method involves adjusting the torque on the turbine shaft in order to set its speed to a reference value. The following relationship allows obtaining a mechanical speed of the generator equal to the reference speed Ω_{ref} using the reference electromagnetic torque C_{em-ref} [55].

$$C_{em-ref} = PI(\Omega_{ref} - \Omega_{mec}) \tag{8}$$

The reference value of the WT speed is the one that corresponds to the optimal value of the speed ratio $\lambda_{Cp\,max}$ (with β constant and equal to 0°), which allows obtaining the maximum value of C_{pmax} as depicted in Figure 2 [56][57].

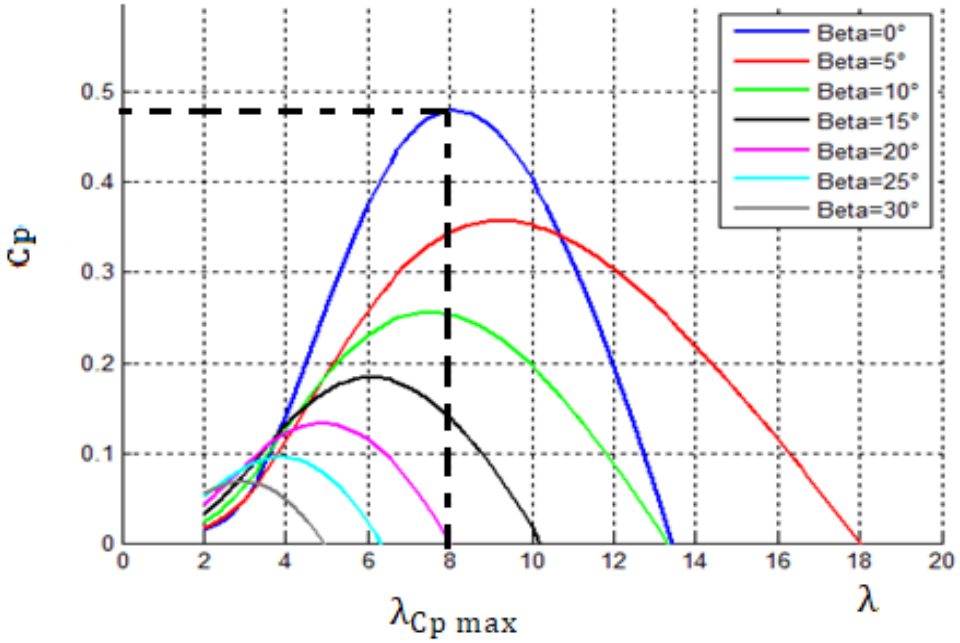


Figure 2. Optimal operation of the WT

It is obtained by inverting equation into:

$$\Omega_{t-ref} = \frac{\lambda_{Cp\,max} \cdot V_1}{R} \tag{9}$$

2.2. Modeling of the DFIM

The Park transformation allows the conversion from a three-phase reference frame to a two-phase model as depicted in Figure 3. It consists of transforming the stator and rotor windings into equivalent orthogonal fictitious windings in order to obtain a mathematical model that is simpler than the physical model of the system [58]-[60].

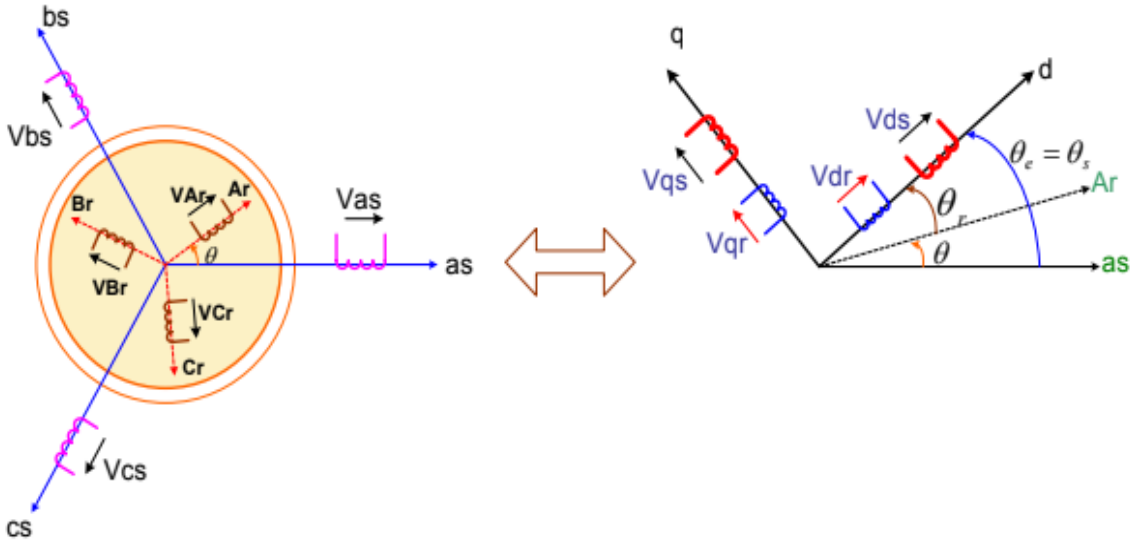


Figure 3. Representation of the transformation $abc \Rightarrow dqo$

In order to implement the principle of vector control, we choose to align the d-axis with the stator flux. The principle of this type of flux orientation is illustrated in Figure 4 [61][62]:

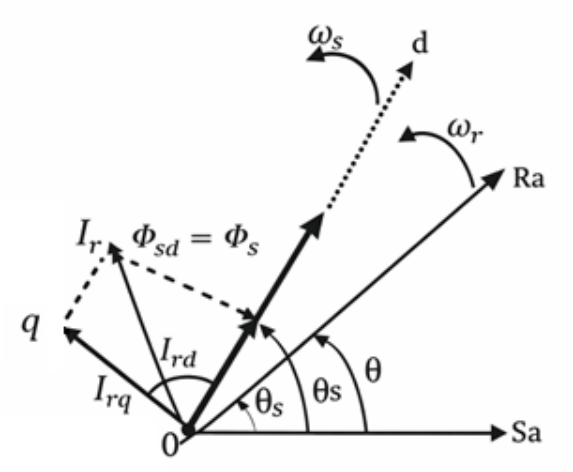


Figure 4. Stator flux orientation

If the resistance of the stator windings is neglected, an assumption often accepted for high-power machines used in wind energy production, the equations of the machine's voltages are reduced to the following form [63][64]:

$$\begin{cases} v_{sd} = 0 \\ v_{sq} = v_s = \omega_s \Phi_s \\ v_{rd} = R_r i_{rd} + \dfrac{d\Phi_{rd}}{dt} - \omega_r \Phi_{rq} \\ v_{rq} = R_r i_{rq} + \dfrac{d\Phi_{rq}}{dt} + \omega_r \Phi_{rd} \end{cases} \quad (10)$$

The expressions for the stator and rotor flux are:

$$\begin{cases} \Phi_{sd} = L_s i_{sd} + M_{sr} i_{rd} \\ 0 = L_s i_{sq} + M_{sr} i_{rq} \end{cases} \quad (11)$$

$$\begin{cases} \Phi_{rd} = L_r i_{rd} + M_{sr} i_{sd} \\ \Phi_{rq} = L_r i_{rq} + M_{sr} i_{sd} \end{cases} \quad (12)$$

Thus, we can express the stator currents in terms of the rotor currents using the expressions for the stator fluxes:

$$\begin{cases} i_{sd} = -\dfrac{M_{sr}}{L_s} i_{rd} + \dfrac{v_s}{\omega_s L_s} \\ i_{sq} = -\dfrac{M_{sr}}{L_s} i_{rq} \end{cases} \quad (13)$$

The expression for the electromagnetic torque then becomes:

$$C_{em} = -P \frac{M_{sr}}{L_s} \Phi_s i_{rq} \quad (14)$$

The operation of the DFIM is similar to that of the DC machine due to this relationship, which resembles the electromagnetic torque of the separately excited DC machine. Assuming that the electrical grid is stable, with a simple voltage vs, this leads to a constant stator flux Φ_s. This consideration, combined with equation, shows that the electromagnetic torque Cem is directly proportional to the rotor current in the quadrature axis. To facilitate the control of energy production by the DFIM, it is convenient to design a model that allows independent control of active and reactive power as depicted in Figure 5. Such a model can be developed by establishing the relationships between active and reactive power, and rotor currents and voltage. In the two-

phase Park frame, the stator active and reactive power of the machine are expressed by the following equations [65]-[68]:

$$\begin{cases} P_s = -v_s \dfrac{M_{sr}}{L_s} i_{rq} \\ Q_s = \left(\dfrac{v_s^2}{L_s \omega_s} - \dfrac{M_{sr}}{L_s} v_s i_{rd}\right) \end{cases} \quad (15)$$

In steady state, the relationship between rotor voltages and currents is as follows [69][70]:

$$\begin{cases} v_{rd} = [R_r + \left(L_r - \dfrac{{M_{sr}}^2}{L_s}\right)P] i_{rd} - g\omega_s \left(L_r - \dfrac{{M_{sr}}^2}{L_s}\right) i_{rq} \\ v_{rq} = [R_r + \left(L_r - \dfrac{{M_{sr}}^2}{L_s}\right)P] i_{rq} + g\omega_s \left(L_r - \dfrac{{M_{sr}}^2}{L_s}\right) i_{rd} + g\dfrac{M_{sr} v_s}{L_s} \end{cases} \quad (16)$$

We can develop the model for power control as presented by the block diagram Figure 5.

The active power for the rotor q-axis and the reactive power for the rotor d-axis will be the reference quantities for these controllers. We will maintain the reference of zero reactive power to ensure a UPF on the stator side, thus improving the quality of the energy sent to the grid. The active power controller will ensure an optimal power transfer from the machine. Thus, there are two methods for performing power control of this machine. The first method involves neglecting the coupling terms and implementing an independent controller on each axis to independently control the active and reactive power as depicted in Figure 6. The second method involves considering the coupling terms and compensating for them by implementing a system with two loops that allow controlling both the powers and the rotor currents.

To regulate the machine, we will implement a control loop on each power with an independent controller while compensating for the disturbance terms present in the block diagram of Figure 6. The low value of the slip will prevent us from considering the coupling terms between the two control axes. It is therefore possible to achieve vector control with a single controller per axis, as illustrated in Figure 7 [71]. The PI controller used to control the DFIM in generator mode is simple and quick to implement while offering acceptable performance [72][73]. A part of our system shows in Figure 7, closed and corrected by a PI controller, whose transfer function is of the form $k_p + \frac{k_i}{s}$ corresponding to the two controllers used in Figure 6. The determination of the parameters kp and ki of the controller involves classical methods for calculating continuous controllers. The design of these controllers is commonly based on classical tuning techniques, among which the ZN oscillation method is one of the most widely used.

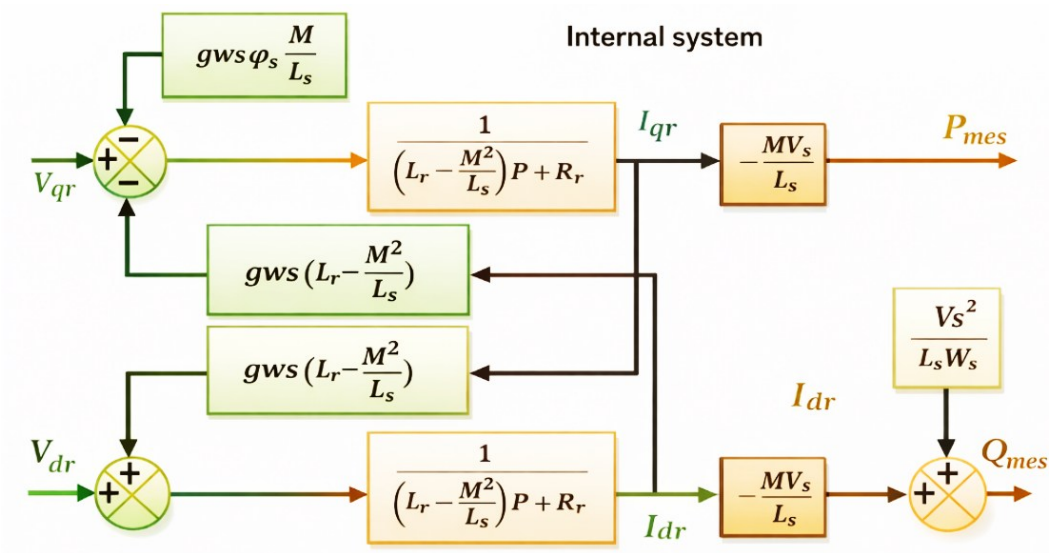


Figure 5. Model of the DFIM for power control

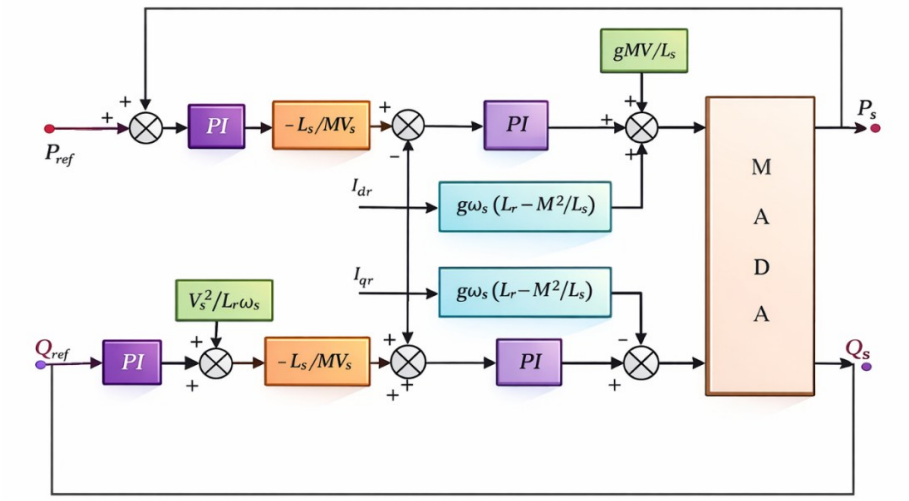


Figure 6. Block diagram of the indirect control with power loop

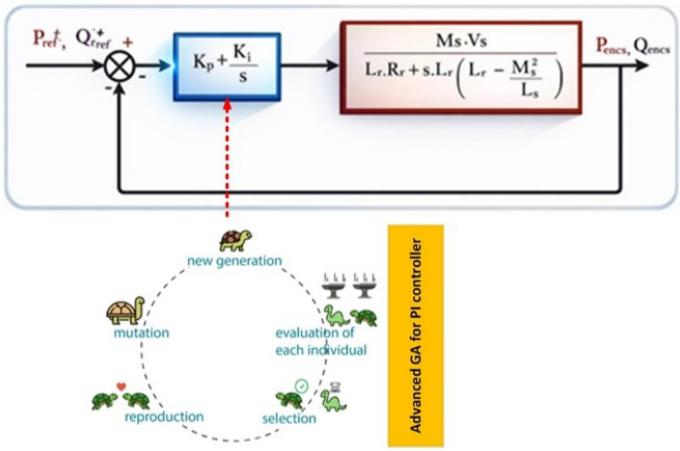


Figure 7. System regulated by a PI controller

3. APPLIED GA TECHNIQUE

Genetic programming is an automatic technique for solving difficult problems by evolving populations of computer programs from one generation to the next. It employs a probabilistic search process which searches over the space of potential combinations of current functions and terminals using guidance from a measure of fitness. The algorithm begins with the generation of a large initial population of randomly constructed programs. Then, using principles drawn from Darwinian natural selection, such as recombination (crossover), mutation, duplication and deletion of genes, and some developmental biology mechanisms, the algorithm continues to enhance the population towards better performing solutions [74][75].

The spirit of genetic programming is three primary steps: Initialization: Generate an initial population made up of various function and terminal combinations relevant to the problem at hand. Evolutionary Loop: (Repeat the following sub-steps collectively called a generation until a termination condition set beforehand is met). Evaluation: (Run each program, then compute a fitness value based on a set performance measure). Selection and Variation: (A new generation is formed by using the following genetic operators probabilistically according to program fitness: Reproduction: Blind copying of good individuals to the next generation. Crossover: Recombination of elements from two parent programs to produce offspring. Mutation: Random alteration of a part of a program to add variation). Architecture-altering operations: (Alterations that reshape the architecture or structure of the programs themselves). Result Designation: The fittest member of the population (in terms of the measure of fitness) is selected as the run output solution. The individual may be an exact or an approximate solution to the problem. The chosen parameters for the genetic algorithm are: (Initial Population = 80, Variable Bounds = [0, 1000], and Maximum Number of Generations = 220). The GA flowchart is seen in Figure 8 [76][77].

A PI controller integrates the most important characteristics of three fundamental control actions: proportional, integral, and derivative. Each makes a different contribution to system performance, and collectively offer greater stability, responsiveness, and steady-state accuracy. A block diagram giving an overview of the control strategy employed in this work is presented in Figure 9.

It can be seen from the diagram that the main purpose of this work is to regulate the PI gain parameters so as to reduce the error between the reference value and the actual output to a minimum. The error signal $e(t)$ is given as the difference between the reference output $r(t)$ and the measured output $y(t)$. The PI control law $u(t)$ is controlled by three parameters: K_p (proportional gain), K_i (integral time). For achievement of such parameters at best operating conditions, appropriate performance indices are desirable. Among the easiest criteria adopted is the ISE, defined mathematically as [78]-[80]:

$$\mathrm{ISE} = \int_0^t \mathrm{e(t)}^2 \mathrm{dt} \tag{17}$$

In this research work, a weighted version of the ISE is employed as the optimisation objective in the GA optimisation scheme. Utilisation of the weighted performance index provides an overall and balanced measure of controller performance, as reported in literature [81][82]. The objective function J used by the GA is defined accordingly in order to drive the search in the direction of the optimal set of PI parameters. The velocity form of the PI control law is used since it is acceptable for real-time implementation and for smooth controller action. The goal is to determine PI parameters that optimize this fitness function over the time interval [0, t]. The algorithm iterates: new generations of PI values hopefully better performing are generated by genetic operators, verified once more, and the cycle repeats. The GA halts when a stopping criterion is met generally, when the difference between fitness value across successive generations falls below a predefined threshold. This repeated process ensures incremental optimization to a point where an optimal or satisfactory set of PI gains is attained.

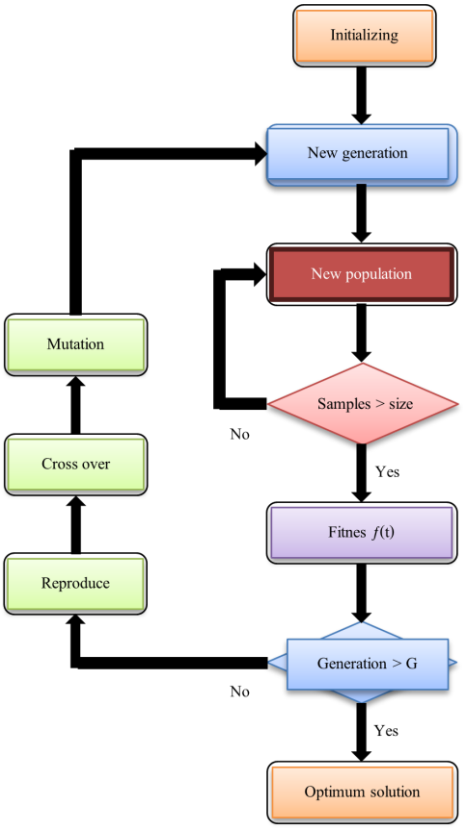


Figure 8. Flowchart of a GA

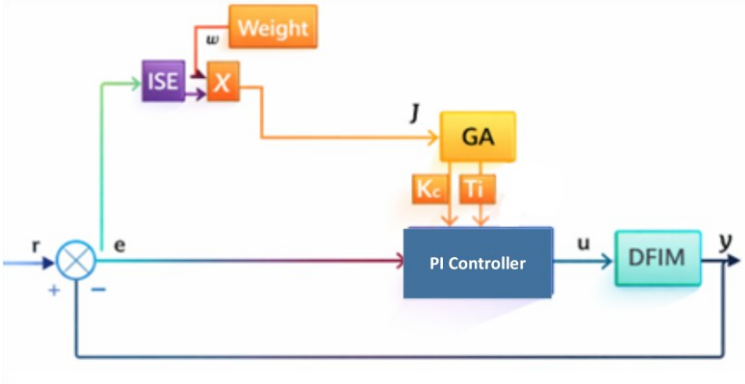


Figure 9. Functional structure of the PI control system

4. RESULTS AND DISCUSSIONS

To verify the effectiveness of the GA in determining the optimal gains and improving the regulation performance of the proposed PI controller, a comparative analysis was carried out between conventionally tuned PI controllers based on manual calculations and GA-optimized PI controllers. The obtained results, illustrated in Figure 10, Figure 11, and Figure 12, demonstrate the capability of the GA approach to identify more suitable controller parameters that enhance the overall dynamic performance of the system. Specifically, Figure 10 presents the PI gain values associated with the speed control loop, highlighting the differences between manually selected gains and those obtained through the optimization process. Figure 11 depicts the optimized and manually calculated PI gains related to the rotor current control loops, showing the effectiveness of GA in achieving better current regulation characteristics. In addition, Figure 12 illustrates the gain values corresponding to the active and reactive power control loops. The comparison confirms that the GA-based tuning method provides more accurate and adaptive gain selection, leading to improved transient response, reduced overshoot, faster settling time, and enhanced stability compared with the manually tuned PI controllers.

The obtained results clearly demonstrate that the GA-based optimization approach provides superior dynamic and steady-state performance compared with the conventional control strategy. The proposed GA tuning method effectively enhances the overall system behavior by achieving a faster transient response, eliminating overshoot, and significantly reducing the steady-state error. In addition, the controller optimized using GA exhibits strong disturbance rejection capability, ensuring stable operation under varying operating conditions and external perturbations.

Figure 13 illustrates the mechanical speed response with and without the implementation of the GA-based controller, where the optimized system achieves rapid tracking with improved stability and reduced oscillations. Figure 14 presents the active power response, highlighting the smoother power regulation and enhanced transient performance obtained using GA optimization. Figure 15 depicts the direct rotor current behavior for both cases, showing that the GA-based controller minimizes current fluctuations and improves current regulation accuracy. Furthermore, Figure 16 shows the electromagnetic torque response, where the optimized controller significantly reduces torque ripples and provides a smoother dynamic response. Overall, the simulation results confirm the effectiveness and robustness of the GA optimization technique in improving the performance of the DFIM control system. Moreover, these simulations have been summarized in Table 3.

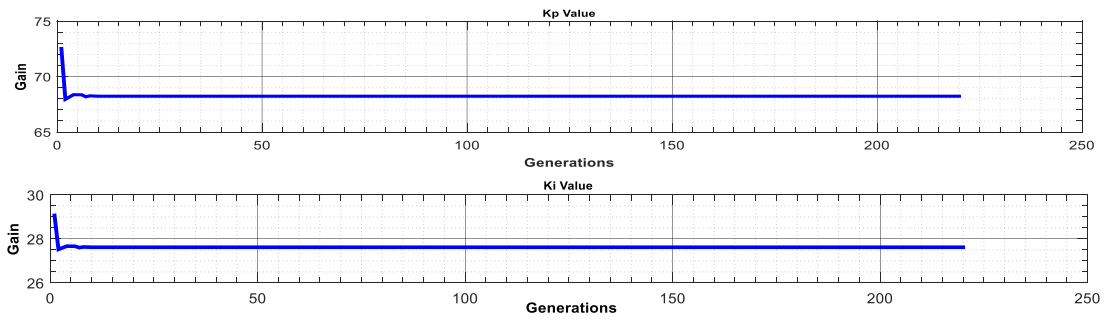


Figure 10. Gain values of the PI for speed

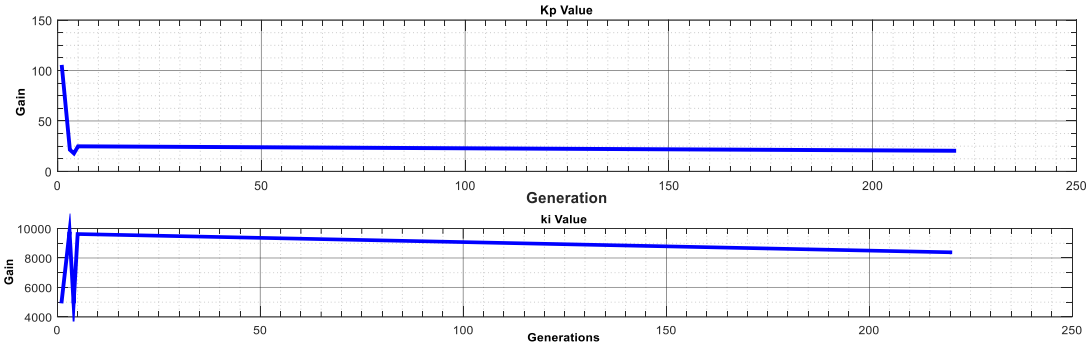


Figure 11. Gain values of the PI for rotor currents

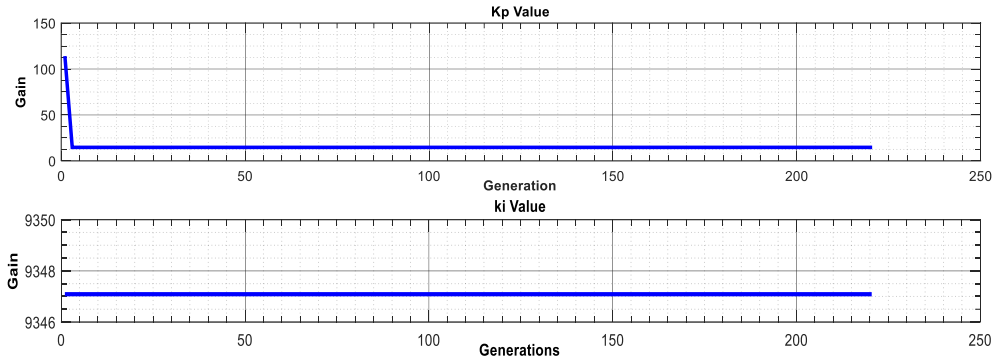


Figure 12. Gain values of the PI for power

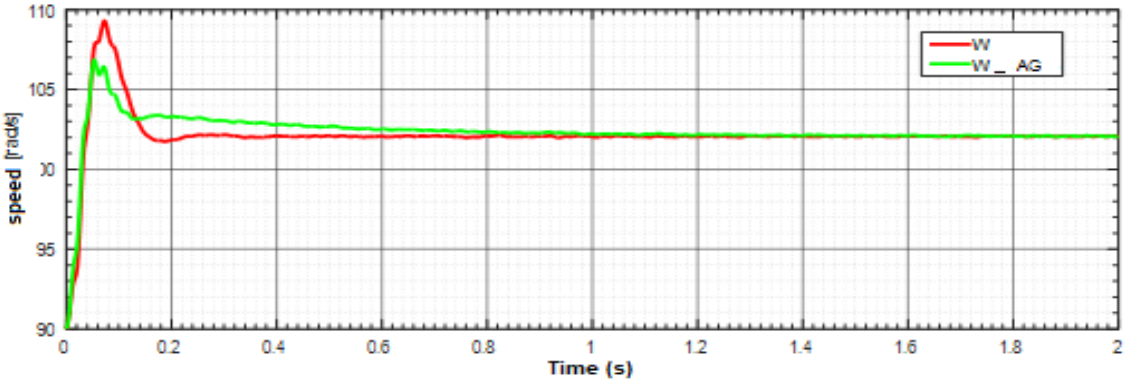


Figure 13. Mechanical speed with and without GA

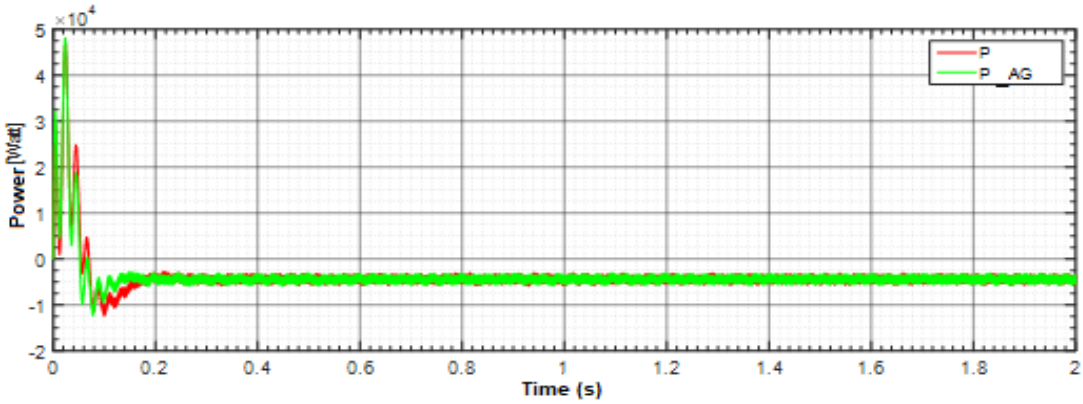


Figure 14. Active power with and without GA application

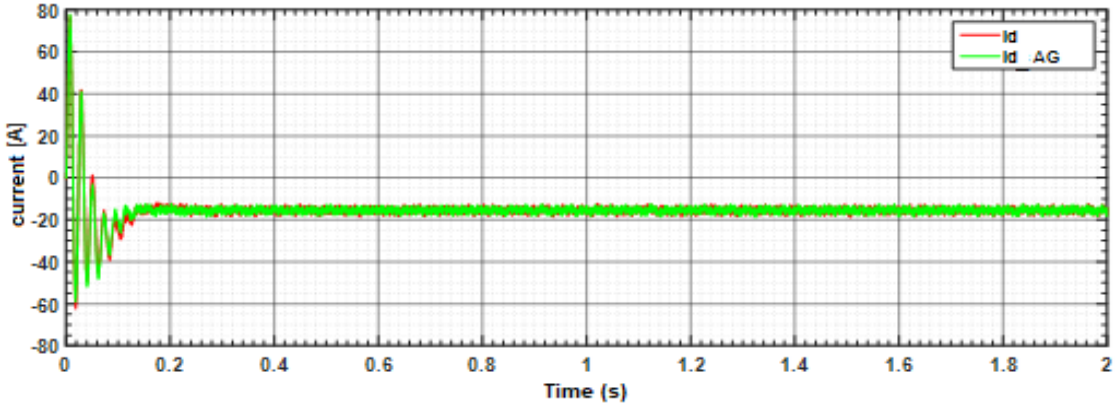


Figure 15. The direct rotor current with and without the application of GA

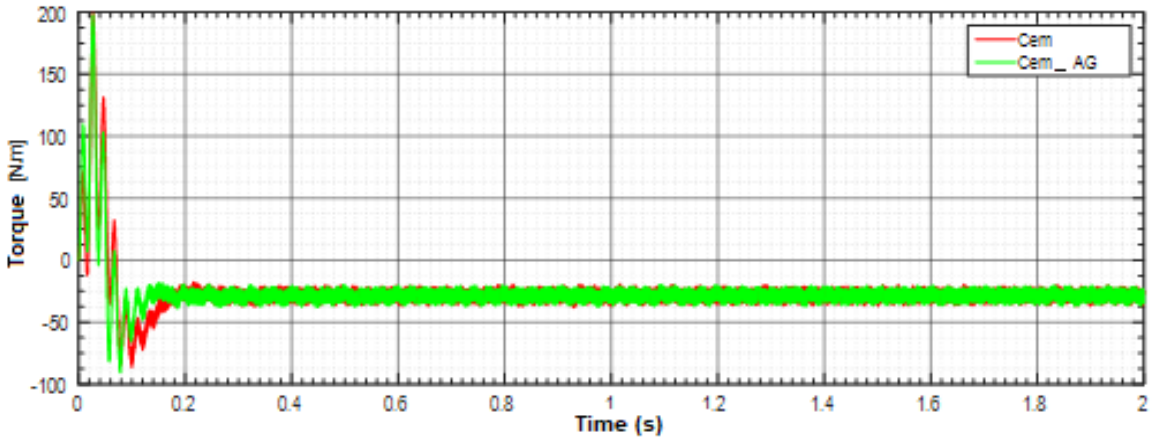


Figure 16. The electromagnetic torque with and without the application of GA

Table 3. Summary of simulated parameters.

Figure	Parameter Evaluated	Performance		Improvement Achieved Using GA
		Without GA	With GA (Proposed)	
Figure 13	Mechanical Speed Response	Slower response with noticeable oscillations and possible overshoot	Faster and smoother response with stable tracking	Reduced settling time, elimination of overshoot, and enhanced stability
Figure 14	Active Power Response	Higher fluctuations and slower stabilization	Smooth and rapid power regulation	Improved transient performance and better power quality
Figure 15	Direct Rotor Current	Current oscillations and less accurate regulation	Stable current profile with reduced fluctuations	Enhanced current regulation accuracy and minimized oscillations
Figure 16	Electromagnetic Torque Response	Significant torque ripples and unstable transient behavior	Smooth torque response with reduced ripples	Improved dynamic performance and enhanced system robustness
Overall Assessment	System Performance	Moderate disturbance rejection with steady-state error	Strong disturbance rejection and minimal steady-state error	Superior dynamic and steady-state performance using GA optimization

5. CONCLUSION

We have successfully enhanced the performance of PI controllers in DFIM using GAs as an optimization technique in this research. The findings of the research indicate that the GA-optimized PI controllers fare significantly better compared to traditionally tuned controllers when it comes to dynamic response, reduction of steady-state error, and overall system stability. Not only does the use of GAs yield better performance values, but it also reduces the level of computation required in performing parameter tuning, making it a viable solution to real-world issues. This contribution highlights the benefit of using GAs as a viable method of optimization for improving control strategies for high-performance electrical drive systems, particularly the utilization of

renewable energy, such as wind energy conversion. By overcoming the nonlinearities and complexities involved in DFIM dynamics, our findings contribute to the work directed towards an improvement in the efficiency and robustness of renewable energy systems. We propose the extension of GA-based optimization techniques to broader applications in the field, as they can facilitate a better performance of control systems in a variety of engineering applications.

DECLARATION

Author Contribution

All authors contributed equally to the main contributor to this paper. All authors read and approved the final paper.

Acknowledgment

This article has been produced with the financial support of the European Union under the REFRESH—Research Excellence For REgion Sustainability and High-tech Industries project number CZ.10.03.01/00/22_003/0000048 via the Operational Programme Just Transition. Also, the authors wish to express their deep gratitude to the Ministry of Higher Education and Scientific Research of Algeria for its essential support in carrying out this study.

Conflicts of Interest

The authors declare no conflict of interest.

List of abbreviations

DFIM	:	doubly-fed induction machine
HAWTs	:	Horizontal-axis wind turbines
MPPT	:	maximum power point tracking
PMSGs	:	permanent magnet synchronous generators
SCIG	:	squirrel cage induction generators
C_p	:	the power coefficient
C_{aer}	:	aerodynamic torque
WECSs	:	Wind energy conversion systems
UPF	:	Unity power factor
WOA	:	Whale optimization algorithm
ABC	:	Artificial bee colony
MPA	:	Marine predators' algorithm
PI	:	proportional-integral
GAs	:	genetic algorithms
PSO	:	particle swarm optimization
FLC	:	fuzzy logic controller
WT	:	wind turbine
β	:	blade pitch angle
λ	:	tip-speed ratio
ZN	:	Ziegler-Nichols
ISE	:	Integral of squared error
DE	:	Differential evolutionary
HHO	:	Harris Hawks Optimization

References

[1] A. Thommessen and C. M. Hackl, "Nonlinear modeling and identification of doubly fed induction machines under varying grid conditions," *IEEE Open J. Ind. Electron. Soc.*, vol. 6, pp. 535–547, 2025, https://doi.org/10.1109/OJIES.2025.3543683.

[2] A. Raj *et al.*, "Adaptive Q-wavelet transform and Kalman filtering for power quality disturbance prediction and carbon emission impact analysis in smart grids," *Eng. Reports*, vol. 8, no. 5, pp. 1–25, 2026, https://doi.org/10.1002/eng2.70825.

[3] H. Guentri, T. Alaoui, V. Blazek, and A. Dahbi, "Robust LQR control design for high efficiency battery supercapacitor hybrid storage systems," *Int. J. Robot. Control Syst.*, vol. 6, no. 2, pp. 1405–1425, 2026, https://doi.org/10.31763/ijrcs.v6i2.1933.

[4] F. Alelaj and A. Alqallaf, "Impact of solar irradiation on the performance ratio of the photovoltaic module," in *Proc. 2019 IEEE 10th GCC Conf. Exhib. (GCC)*, 2019, https://doi.org/10.1109/GCC45510.2019.9087579.
[5] F. Alelaj and A. Alqallaf, "Optimization of the tilt angle of the photo-voltaic module in Kuwait," in *Proc. 2019 IEEE 10th GCC Conf. Exhib. (GCC)*, 2019, https://doi.org/10.1109/GCC45510.2019.1570525127.
[6] A. T. Hassan *et al.*, "Intelligent chopper and RSC control using crayfish optimization for dynamic stability and fault ride-through of DFIG wind turbines," *Int. J. Robot. Control Syst.*, vol. 6, no. 1, pp. 693–717, 2026, https://doi.org/10.31763/ijrcs.v6i1.2002.
[7] S. Heroual *et al.*, "Genetic algorithm tuned controllers for high-performance indirect field-oriented control in DFIG-based WECS," *Bul. Ilm. Sarj. Tek. Elektro*, vol. 8, no. 1, pp. 294–310, 2026, https://doi.org/10.12928/biste.v8i1.15529.
[8] N. M. Tahir, A. Y. Babawuro, F. M. Alelaj, B. B. Muhammad, S. S. Shitu, and I. A. Umar, "Control of a single-link flexible manipulator: Integration of output-based filter with model predictive constraint," *J. Phys. Conf. Ser.*, vol. 3191, no. 1, p. 012043, 2026, https://doi.org/10.1088/1742-6596/3191/1/012043.
[9] M. T. Mohamed *et al.*, "Intelligent frequency regulation in islanded microgrids using a crayfish-tuned FO–(PD–PI) controller with energy storage coordination," *J. Low Freq. Noise Vib. Act. Control*, vol. 0, no. 0, pp. 1–32, 2026, https://doi.org/10.1177/14613484261429576.
[10] M. Miloudi *et al.*, "Comprehensive experimental performance investigation of conducted electromagnetic interference in split-phase induction motors: Common-mode," *J. Low Freq. Noise Vib. Act. Control*, vol. 0, no. 0, pp. 1–20, 2026, https://doi.org/10.1177/14613484251411703.
[11] A. Carreno, M. A. Perez and M. Malinowski, "State-Feedback Control of a Hybrid Distribution Transformer for Power Quality Improvement of a Distribution Grid," in *IEEE Transactions on Industrial Electronics*, vol. 71, no. 2, pp. 1147-1157, Feb. 2024, https://doi.org/10.1109/TIE.2023.3262872.
[12] M. Tarek and M. I. M. Elzein, "Sustainable energy management in islanded microgrids via HHO – BE tuned adaptive controllers and demand-side flexibility," *Eng. Reports*, vol. 8, no. 1, pp. 1–20, 2026, https://doi.org/10.1002/eng2.70561.
[13] S. Nadweh, I. M. Elzein, D. E. M. Wapet, and M. M. M. Benameur, "Optimizing control of single-ended primary inductor converter integrated with microinverter for PV systems: Imperialist competitive algorithm," *Energy Explor. Exploit.*, 2025, https://doi.org/10.1177/01445987251382002.
[14] M. A. Bou-Rabee, F. M. Alelaj, and H. Al-Sairfi, "Quantifying the economic loss and operational implications of air pollution on grid-connected PV systems in the Arabian Peninsula: A machine learning-based analysis," *IEEE Access*, vol. 14, pp. 4180–4188, 2026, https://doi.org/10.1109/ACCESS.2025.3649764.
[15] D. Cui *et al.*, "Enhancing short-term electricity forecasting with advanced machine learning techniques," *J. Electr. Eng. Technol.*, 2025, https://doi.org/10.1007/s42835-025-02430-z.
[16] N. V. A. Ravikumar *et al.*, "Design and real-time simulations of robust controllers for uncertain multi-input wind turbine," *Energy Explor. Exploit.*, vol. xx, no. xx, p. xx, 2025, https://doi.org/10.1177/01445987251373101.
[17] P. Sinha *et al.*, "Efficient automated detection of power quality disturbances using nonsubsampled contourlet transform & PCA-SVM," *Energy Explor. Exploit.*, vol. 00, no. 00, 2025, https://doi.org/10.1177/01445987241312755.
[18] A. M. E. A. Raj *et al.*, "Wavelet Analysis- Singular Value Decomposition Based Method for Precise Fault Localization in Power Distribution Networks Using k-NN Classifier," *Int. J. Robot. Control Syst.*, vol. 5, no. 1, pp. 530–554, 2025, https://doi.org/10.31763/ijrcs.v5i1.1543.
[19] M. Basu *et al.*, "Flexible dynamic optimal power flow integrating renewable energy sources and electric vehicle parking IOT," *Eng. Reports*, vol. 7, no. 12, 2025, https://doi.org/10.1002/eng2.70568.
[20] N. F. Ibrahim *et al.*, "Enhanced control of single-stage PV-STATCOM using hybrid MPPT and adaptive AHLMS for power quality improvement," *IEEE Access*, vol. 13, pp. 200253–200270, 2025, https://doi.org/10.1109/ACCESS.2025.3635707.
[21] A. Fayz *et al.*, "Optimal controller design of crowbar system for DFIG-based WT: Applications of Gravitational Search Algorithm," *Bul. Ilm. Sarj. Tek. Elektro*, vol. 7, no. 2, pp. 122–136, 2025, https://doi.org/10.12928/biste.v7i2.13027.
[22] T. Boutabba *et al.*, "Design of a small wind turbine emulator for testing power converters using dSPACE 1104," *Int. J. Robot. Control Syst.*, vol. 5, no. 2, pp. 698–712, 2025, https://doi.org/10.31763/ijrcs.v5i2.1685.
[23] W. Fendzi *et al.*, "Policy-driven expansion of renewable energy in Cameroon: A technical and sustainability-centered analysis of growth trends and cross-sectoral impacts (2015–2024)," *Energy Strateg. Rev.*, vol. 62, p. 101912, 2025, https://doi.org/10.1016/j.esr.2025.101912.
[24] H. Abdelfattah *et al.*, "Supporting the reactivity of nuclear power plants using an optimized FOPID controller with arithmetic algorithm: Toward an environmentally sustainable energy system," *Energy Explor. Exploit.*, 2025, https://doi.org/10.1177/01445987251357362.
[25] A. Hysa *et al.*, "Advanced modeling and comparative error analysis of photovoltaic cells using multi-diode models and EQE characterization," *Int. J. Robot. Control Syst.*, vol. 6, no. 5, pp. 2308–2321, 2025, https://doi.org/10.18196/jrc.v6i5.27539.

[26] I. M. Elzein *et al.*, "The utilization of a TSR-MPPT-based backstepping controller and speed estimator across varying intensities of wind speed turbulence," *Int. J. Robot. Control Syst.*, vol. 5, no. 2, pp. 1315–1330, 2025, https://doi.org/10.31763/ijrcs.v5i2.1793.
[27] P. Sinha *et al.*, "Classifying power quality issues in railway electrification systems using a nonsubsampled contourlet transform approach," *Eng. Reports*, vol. 7, no. 8, 2025, https://doi.org/10.1002/eng2.70301.
[28] R. Bousseksou *et al.*, "Utilizing Short-Time Fourier Transform for the Diagnosis of Rotor Bar Faults in Induction Motors Under Direct Torque Control," *Int. J. Robot. Control Syst.*, vol. 5, no. 2, pp. 1441–1457, 2025, https://doi.org/10.31763/ijrcs.v5i2.1886.
[29] S. Basu *et al.*, "Applications of Snow Ablation Optimizer for Sustainable Dynamic Dispatch of Power and Natural Gas Assimilating Multiple Clean Energy Sources," *Eng. Reports*, vol. 7, no. 6, pp. 1–12, 2025, https://doi.org/10.1002/eng2.70211.
[30] O. M. Kamel *et al.*, "Effective energy management strategy with a novel design of fuzzy logic and JAYA-based controllers in isolated DC/AC microgrids: A comparative analysis," *Wind Eng.*, vol. 49, no. 1, pp. 199–222, 2025, https://doi.org/10.1177/0309524X241263518.
[31] S. Heroual *et al.*, "Optimizing Power Flow in Photovoltaic-Hybrid Energy Storage Systems: A PSO and DPSO Approach for PI Controller Tuning," *Int. Trans. Electr. Energy Syst.*, vol. 2025, no. 1, p. 9958218, 2025, https://doi.org/10.1155/etep/9958218.
[32] Y. Maamar *et al.*, "Design, Modeling, and Simulation of A New Adaptive Backstepping Controller for Permanent Magnet Linear Synchronous Motor: A Comparative Analysis," *Int. J. Robot. Control Syst.*, vol. 5, no. 1, pp. 296–310, 2025, https://doi.org/10.31763/ijrcs.v5i1.1425.
[33] A. Alkuhayli, U. Khaled, and M. M. Mahmoud, "A novel hybrid Harris Hawk optimization – sine cosine transmission network," *Energies*, vol. 17, no. 19, p. 4985, 2024, https://doi.org/10.3390/en17194985.
[34] R. Bhol *et al.*, "Performance analysis of DFIG support microgrid using GA optimized restricted Boltzmann Machine algorithm," *Heliyon*, vol. 10, no. 10, p. e30669, 2024, https://doi.org/10.1016/j.heliyon.2024.e30669.
[35] C. Lotfi *et al.*, "Optimization of a speed controller of a DFIM with metaheuristic algorithms," *Eng. Proc.*, vol. 29, no. 1, p. 29013, 2023, https://doi.org/10.3390/engproc2023029013.
[36] J. He *et al.*, "Quantification of wind farm stabilization areas with the Grey Wolf Optimizer and Support Vector Machine," in *Proc. 2025 10th Asia Conf. Power Electrical Eng. (ACPEE)*, pp. 1168–1174, 2025, https://doi.org/10.1109/ACPEE64358.2025.11040248.
[37] A. S. Kumar, D. R. Kishore, K. P. Kumar, S. Sriram, and P. Vamsi, "Whale optimization-based PI control for DFIG wind energy systems with modular multilevel grid-side converter," *Int. J. Smart Grid*, vol. 9, no. 2, pp. 94–104, 2025, https://doi.org/10.20508/ijsmartgrid.v9i2.413.g384.
[38] O. M. Kamel, A. A. Z. Diab, T. D. Do, and M. A. Mossa, "A novel hybrid ant colony-particle swarm optimization techniques based tuning STATCOM for grid code compliance," *IEEE Access*, vol. 8, pp. 41566–41587, 2020, https://doi.org/10.1109/ACCESS.2020.2976828.
[39] H. K. R. Alluri, A. S. L. V. Tummala, P. V. Ramanarao, and P. V. N. Mohan Krishna, "Optimal tuning of PI controllers for DFIG-based wind energy system using self-adaptive differential evolution algorithm," *Int. J. Electr. Eng. Informatics*, vol. 11, no. 2, pp. 352–372, 2019, https://doi.org/10.15676/ijeei.2019.11.2.9.
[40] D. Kumar and K. Chatterjee, "Design and analysis of artificial bee-colony-based MPPT algorithm for DFIG-based wind energy conversion systems," *Int. J. Green Energy*, vol. 14, no. 4, pp. 416–429, 2017, https://doi.org/10.1080/15435075.2016.1261709.
[41] I. Katib and M. Ragab, "Blockchain-assisted hybrid Harris hawks optimization based deep DDoS attack detection in the IoT environment," *Mathematics*, vol. 11, no. 8, p. 1887, 2023, https://doi.org/10.3390/math11081887.
[42] R. G. Mohamed, M. A. Ebrahim, Z. M. Alaas, and M. M. R. Ahmed, "Optimal energy harvesting of large-scale wind farm using Marine Predators Algorithm," *IEEE Access*, vol. 10, pp. 24995–25004, 2022, https://doi.org/10.1109/ACCESS.2022.3156084.
[43] M. Guediri, A. Guediri, N. Ikhlef, B. Hocine, and A. Guediri, "Optimization by genetic algorithm of a wind energy system applied to a dual-feed generator," *Eng. Technol. Appl. Sci. Res.*, vol. 14, no. 5, pp. 16890–16896, 2024, https://doi.org/10.48084/etasr.8122.
[44] H. Boudjemai *et al.*, "Design, simulation, and experimental validation of a new fuzzy logic-based maximal power point tracking strategy for low power wind turbines," *Int. J. Fuzzy Syst.*, vol. 5, no. 1, pp. 296–310, 2025, https://doi.org/10.31763/ijrcs.v5i1.1425.
[45] B. K. Ponukumati *et al.*, "Evolving fault diagnosis scheme for unbalanced distribution network using fast normalized cross-correlation technique," *PLoS One*, vol. 19, no. 10, p. e0305407, 2024, https://doi.org/10.1371/journal.pone.0305407.
[46] D. Assessment and C. Defect, "Dynamic assessment and control of a dual star induction machine state dedicated to an electric vehicle under short-circuit defect," *Int. J. Robot. Control Syst.*, vol. 4, no. 4, pp. 1731–1745, 2024.
[47] F. Menzri *et al.*, "Applications of novel combined controllers for optimizing grid-connected hybrid renewable energy systems," *Sustainability*, vol. 16, no. 16, p. 6825, 2024, https://doi.org/10.3390/su16166825.
[48] H. Alnami, S. A. E. M. Ardjoun, and M. M. Mahmoud, "Design, implementation, and experimental validation of a new low-cost sensorless wind turbine emulator: Applications for small-scale turbines," *Wind Eng.*, vol. 48, no. 4, pp. 565–579, 2024, https://doi.org/10.1177/0309524X231225776.

[49] B. S. Atia *et al.*, "Applications of Kepler algorithm-based controller for DC chopper: Towards stabilizing wind driven PMSGs under nonstandard voltages," *Sustainability*, vol. 16, no. 7, p. 2952, 2024, https://doi.org/10.3390/su16072952.
[50] M. Chebaani, M. M. Mahmoud, A. F. Tazay, M. I. Mosaad, and N. A. Nouraldin, "Extended Kalman Filter design for sensorless sliding mode predictive control of induction motors without weighting factor: An experimental investigation," *PLoS One*, vol. 18, no. 11, p. e0293278, 2023, https://doi.org/10.1371/journal.pone.0293278.
[51] N. F. Ibrahim *et al.*, "Multiport converter utility interface with a high-frequency link for interfacing clean energy sources (PV\Wind\Fuel Cell) and battery to the power system: Application of the HHA algorithm," *Sustainability*, vol. 15, no. 18, p. 13716, 2023, https://doi.org/10.3390/su151813716.
[52] H. Boudjemai *et al.*, "Experimental analysis of a new low power wind turbine emulator using a DC machine and advanced method for maximum wind power capture," *IEEE Access*, vol. 11, pp. 93308–93319, 2023, https://doi.org/10.1109/ACCESS.2023.3308040.
[53] S. Ashfaq *et al.*, "Comparing the role of long duration energy storage technologies for zero-carbon electricity systems," *IEEE Access*, vol. 12, pp. 73169–73186, 2024, https://doi.org/10.1109/ACCESS.2024.3397918.
[54] M. M. Hussein *et al.*, "Regulation of multi-area power system load frequency in presence of V2G scheme," *PLoS One*, vol. 18, no. 9, p. e0291463, 2023, https://doi.org/10.1371/journal.pone.0291463.
[55] A. H. Elmetwaly *et al.*, "Modeling, simulation, and experimental validation of a novel MPPT for hybrid renewable sources integrated with UPQC: An application of Jellyfish Search Optimizer," *Sustainability*, vol. 15, no. 6, p. 5209, 2023, https://doi.org/10.3390/su15065209.
[56] H. Boudjemai *et al.*, "Application of a novel synergetic control for optimal power extraction of a small-scale wind generation system with variable loads and wind speeds," *Symmetry*, vol. 15, no. 2, p. 369, 2023, https://doi.org/10.3390/sym15020369.
[57] N. A. N. Aldin, W. S. E. Abdellatif, Z. M. S. Elbarbary, A. I. Omar, and M. M. Mahmoud, "Robust speed controller for PMSG wind system based on Harris Hawks optimization via wind speed estimation: A real case study," *IEEE Access*, vol. 11, pp. 4320–4332, 2023, https://doi.org/10.1109/ACCESS.2023.3234996.
[58] M. M. Mahmoud *et al.*, "Integration of wind systems with SVC and STATCOM during various events to achieve FRT capability and voltage stability: Towards the reliability of modern power systems," *Int. J. Energy Res.*, vol. 2023, p. 8738460, 2023, https://doi.org/10.1155/2023/8738460.
[59] M. M. Mahmoud *et al.*, "Evaluation and comparison of different methods for improving fault ride-through capability in grid-tied permanent magnet synchronous wind generators," *Int. Trans. Electr. Energy Syst.*, vol. 2023, p. 7717070, 2023, https://doi.org/10.1155/2023/7717070.
[60] A. Mitrovic, L. Strezoski, and K. A. Loparo, "Doubly fed induction machine models for integration into grid management software for improved post fault response calculation accuracy—A short review," *Energies*, vol. 18, no. 1, p. 147, 2025, https://doi.org/10.3390/en18010147.
[61] M. M. Mahmoud, B. S. Atia, A. Y. Abdelaziz, and N. A. N. Aldin, "Dynamic performance assessment of PMSG and DFIG-based WECS with the support of Manta Ray Foraging Optimizer considering MPPT, pitch control, and FRT capability issues," *Processes*, vol. 12, no. 10, p. 2723, 2022, https://doi.org/10.3390/pr12102723.
[62] A. Glazyrin *et al.*, "Nonlinear algebraic parameter estimation of doubly fed induction machine based on rotor current falling curves," *Energies*, vol. 18, no. 16, p. 4316, 2025, https://doi.org/10.3390/en18164316.
[63] M. M. Mahmoud, M. M. Aly, H. S. Salama, and A. M. M. Abdel-Rahim, "A combination of an OTC based MPPT and fuzzy logic current control for a wind-driven PMSG under variability of wind speed," *Energy Syst.*, vol. 13, no. 4, pp. 1075–1098, 2022, https://doi.org/10.1007/s12667-021-00468-2.
[64] M. M. Mahmoud, M. K. Ratib, M. M. Aly, and A. M. M. Abdel–Rahim, "Application of Whale Optimization Technique for Evaluating the Performance of Wind-Driven PMSG Under Harsh Operating Events," *Process Integr. Optim. Sustain.*, 2022, https://doi.org/10.1007/s41660-022-00224-8.
[65] M. M. Mahmoud, M. M. Aly, H. S. Salama, and A.-M. M. Abdel-Rahim, "An internal parallel capacitor control strategy for DC-link voltage stabilization of PMSG-based wind turbine under various fault conditions," *Wind Eng.*, vol. 46, no. 4, pp. 450–462, 2021, https://doi.org/10.1177/0309524X211060684.
[66] M. M. Mahmoud, M. K. Ratib, M. M. Aly, and A. M. M. Abdel-Rahim, "Wind-driven permanent magnet synchronous generators connected to a power grid: Existing perspective and future aspects," *Wind Eng.*, vol. 46, no. 1, pp. 189–199, 2022, https://doi.org/10.1177/0309524X211022728.
[67] M. M. Mahmoud *et al.*, "Voltage Quality Enhancement of Low-Voltage Smart Distribution System Using Robust and Optimized DVR Controllers: Application of the Harris Hawks Algorithm," *Int. Trans. Electr. Energy Syst.*, vol. 2022, p. 4242996, 2022, https://doi.org/10.1155/2022/4242996.
[68] M. M. Mahmoud, M. K. Ratib, I. J. Raglend, J. Swaminathan, M. M. Aly, and A. M. M. Abdel-Rahim, "Application of Grey Wolf Optimization for PMSG-Based WECS under Different Operating Conditions: Performance Assessment," in *Proc. 3rd IEEE Int. Virtual Conf. Innovations Power Adv. Comput. Technol. (i-PACT)*, 2021, https://doi.org/10.1109/i-PACT52855.2021.9696881.
[69] M. M. Mahmoud, H. S. Salama, M. M. Aly, and A. M. M. Abdel-Rahim, "Design and implementation of FLC system for fault ride-through capability enhancement in PMSG-wind systems," *Wind Eng.*, vol. 45, no. 5, pp. 1361–1373, 2021, https://doi.org/10.1177/0309524X20981773.

[70] M. M. Mahmoud, M. M. Aly, H. S. Salama, and A. M. M. Abdel-Rahim, "Dynamic evaluation of optimization techniques–based proportional–integral controller for wind-driven permanent magnet synchronous generator," *Wind Eng.*, vol. 45, no. 3, pp. 696–709, 2021, https://doi.org/10.1177/0309524X20930421.
[71] G. Dauksha, D. Górski, and G. Iwański, "State-feedback control of a grid-tied cascaded brushless doubly-fed induction machine," *Electr. Power Syst. Res.*, vol. 228, p. 110043, 2024, https://doi.org/10.1016/j.epsr.2023.110043.
[72] A. Thommessen and C. M. Hackl, "Virtual Synchronous Machine Control for Doubly Fed Induction Machine-Based Wind Energy Conversion Systems," *IEEE Open J. Ind. Electron. Soc.*, vol. 5, pp. 264–301, 2024, https://doi.org/10.1109/OJIES.2024.3366082.
[73] Z. Zheng *et al.*, "Model Reference Adaptive Sensorless Control of Variable-Speed Pumped Storage Doubly Fed Induction Machine Under Reversible Operations," *Energies*, vol. 18, no. 11, p. 2998, 2025, https://doi.org/10.3390/en18112998.
[74] S. Katoch, S. S. Chauhan, and V. Kumar, "A review on genetic algorithm: past, present, and future," *Multimed. Tools Appl.*, vol. 80, no. 5, pp. 8091–8126, 2021, https://doi.org/10.1007/s11042-020-10139-6.
[75] B. Alhijawi and A. Awajan, "Genetic algorithms: theory, genetic operators, solutions, and applications," *Evolutionary Intelligence*, vol. 17, no. 3, pp. 1245–1256, 2024, https://doi.org/10.1007/s12065-023-00822-6.
[76] W. H. Lam, W. S. Lam, and P. F. Lee, "A Bibliometric Analysis of a Genetic Algorithm for Supply Chain Agility," *Mathematics*, vol. 12, no. 8, p. 1199, 2024, https://doi.org/10.3390/math12081199.
[77] M. A. Londe, L. S. Pessoa, C. E. Andrade, and M. G. C. Resende, "Biased random-key genetic algorithms: A review," *Eur. J. Oper. Res.*, vol. 321, no. 1, pp. 1–22, 2025, https://doi.org/10.1016/j.ejor.2024.03.030.
[78] F. M. Isa, W. N. M. Ariffin, M. S. Jusoh, and E. P. Putri, "A review of genetic algorithm: Operations and applications," *J. Adv. Res. Appl. Sci. Eng. Technol.*, vol. 40, no. 1, pp. 1–34, 2024, https://doi.org/10.37934/araset.40.1.134.
[79] R. Medel-Esquivel, I. Gómez-Vargas, A. A. M. Sánchez, R. García-Salcedo, and J. A. Vázquez, "Cosmological parameter estimation with genetic algorithms," *Universe*, vol. 10, no. 1, p. 11, 2024, https://doi.org/10.3390/universe10010011.
[80] M. Fadel and H. Al Sairfi, "Adaptive fuzzy energy management of wind-battery systems with flexible desalination load," *Energy Sci. Eng.*, vol. 0, no. 0, pp. 1–17, 2026, https://doi.org/10.1002/ese3.70570.
[81] Y. Pan *et al.*, "A review of hybrid vehicles classification and their energy management strategies: An exploration of the advantages of genetic algorithms," *Algorithms*, vol. 18, no. 6, p. 354, 2025, https://doi.org/10.3390/a18060354.
[82] H. Nematzadeh, J. García-Nieto, S. Hurtado, J. F. Aldana-Montes, and I. Navas-Delgado, "Model-agnostic local explanation: Multi-objective genetic algorithm explainer," *Eng. Appl. Artif. Intell.*, vol. 139, p. 109628, 2025, https://doi.org/10.1016/j.engappai.2024.109628.